

## Revisiting the Mechanism of the Unimolecular Fragmentation of Protonated Fluorobenzene

Detlef Schröder,<sup>\*,†</sup> Izhack Oref,<sup>\*,‡</sup> Jan Hrušák,<sup>\*,§</sup> Thomas Weiske,<sup>†</sup> Evgueni E. Nikitin,<sup>‡</sup> Waltraud Zummack,<sup>†</sup> and Helmut Schwarz<sup>†</sup>

*Institut für Organische Chemie der Technischen Universität Berlin, D-10623 Berlin, Germany, the Department of Chemistry, Technion—Israel Institute of Technology, Haifa 32000, Israel, and the Academy of Sciences of the Czech Republic, J. Heyrovsky Institute of Physical Chemistry, Cz-18223 Prague 8, Czech Republic*

Received: February 22, 1999

The composite kinetic energy release (KER) associated with the decomposition of metastable, protonated fluorobenzene is examined in detail by means of mass spectrometry and analyzed theoretically using a combination of RRKM theory and the statistical adiabatic channel model (SACM). A model for the KER is presented, and contributions of rotational, vibrational, and zero-point energies are calculated. The predictions are in reasonable agreement with the experimentally measured data for two of three components of the KER. With respect to the third, the results lead to a reconsideration of earlier mechanistic models and indicate that ring-opening may occur during the unimolecular decomposition of protonated fluorobenzene. This hypothesis is supported by the ion/molecule reactions of  $C_6H_5^+$  cations formed by dissociative protonation of fluorobenzene with strong Brønsted acids.

## Introduction

Thermodynamic and kinetic aspects in the protonation of arenes are of ongoing interest in ion chemistry in general and for physical organic chemistry in particular.<sup>1</sup> Besides the recently revived discussion on the stability of  $\sigma$ - and  $\pi$ -protonated benzene,<sup>2–4</sup> the gas-phase protonation of mono-<sup>5–8</sup> and poly-fluorobenzenes<sup>6,9,10</sup> has attracted particular attention. When produced by chemical ionization with strong Brønsted acids, e.g.,  $H_3^+$  or  $CH_5^+$ , protonated fluorobenzene undergoes unimolecular dehydrofluorination, i.e.,  $[C_6H_5F \cdot H^+] \rightarrow C_6H_5^+ + HF$ . In 1993, some of us proposed a mechanism for this fragmentation, according to which of the ring-protonated isomers **1–4** (Scheme 1) decay via two different routes involving the transition structures **5** and **6** (Figure 1).<sup>11</sup> Both channels led to the same intermediate **7** and identical dissociation products, namely phenyl cation<sup>12</sup> and neutral HF. The different kinetic energy releases (KERs) associated with the formation of  $C_6H_5^+$  observed experimentally were attributed to dissociation of the competing channels via **5** and **6**.

The two pieces of evidence that led to the previously suggested mechanism<sup>11</sup> shall be reviewed briefly. (i) The unimolecular loss of HF from  $[C_6H_5F \cdot H^+]$  is associated with three different KERs; these components are sketched in Figure 2. The narrowest component of the KER with  $T_{0.5} = 1.3$  meV ( $T_{0.5}$  stands for the KER at half-height of the peak)<sup>13,14</sup> was unequivocally attributed to the unimolecular decay of metastable **7** by means of isotopic labeling and is only observed if the protonation agent used in chemical ionization closely matches the proton affinity of the fluorine atom in fluorobenzene. The remaining medium and broad components of the KER ( $T_{0.5} = 16$  and 424 meV, respectively) are observed with a series of protonating agents and involve the ring-protonated species **1–4**. (ii) Ab initio MO calculations at various levels of theory predict

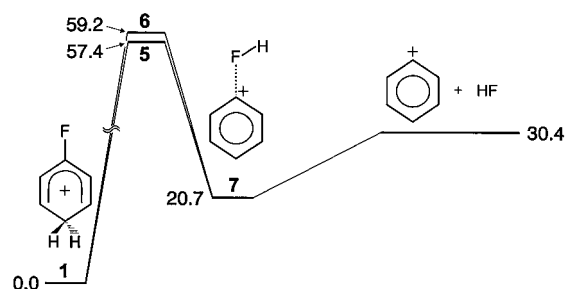
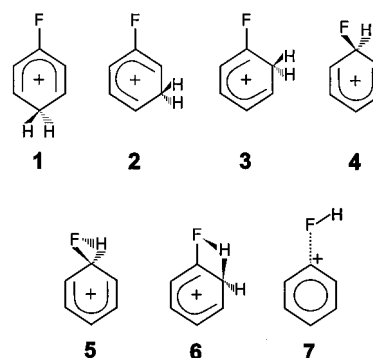


**Figure 1.** Schematic potential-energy surface for the HF loss from protonated fluorobenzene according to the ab initio calculations reported in ref 11; note that **1** is connected with **5** and **6**, respectively, via a sequence of 1,2-H migrations. Relative energies are given in kcal/mol.

## SCHEME 1



that the activation barriers for unimolecular HF losses via **5** and **6**, respectively, are very close in energy (e.g.,  $\Delta E = 2.1$  kcal/mol at MP2/6-31G\*\*//HF/6-31G\*). Therefore, direct competition between both channels in metastable ion dissociation was considered to be feasible. The central hypothesis was that these two pathways are associated with different KERs because of different energy partitioning in the product modes.<sup>13,15</sup>

Before proceeding, let us consider some more general aspects of KER which are relevant for the  $[C_6H_5F \cdot H^+]$  system. When

<sup>†</sup> Technical University of Berlin; fax (+) 49 30 314 21102.

<sup>‡</sup> Technion; fax (+) 972-4 8233735.

<sup>§</sup> J. Heyrovsky Institute of Physical Chemistry.

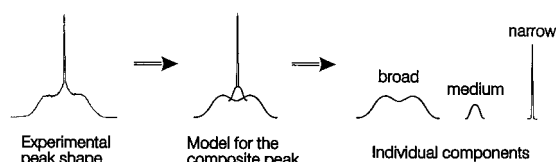


**Figure 2.** Schematic deconvolution of the experimentally obtained composite peak associated with unimolecular loss of HF from  $[\text{C}_6\text{H}_5\text{F}\cdot\text{H}^+]$  generated by chemical ionization of fluorobenzene with methane as reagent gas; for further details, see ref 11.

a diatomic molecule is formed in the unimolecular decomposition of a metastable, polyatomic precursor with statistical behavior, its distribution function  $\varphi$  over translational, rotational, and vibrational states is determined by two phenomena, i.e., the statistical redistribution of energy in the TS and the interaction between the different modes in the exit channels en route to dissociation. A priori calculation of distribution functions is difficult, because it requires a combined treatment of the statistical and dynamic regimes. Two theories exist that allow for a simplified description of unimolecular decompositions and the associated KERs. The first is phase-space theory (PST),<sup>16</sup> which is based upon the assumption that the interaction in the exit channels can be described by a statistical approach. Therefore,  $\varphi$  of a fragment is just a statistical distribution function calculated under two constraints, namely, conservation of energy and angular momentum. The second theory is the statistical adiabatic channel model (SACM),<sup>17</sup> which assumes that the system evolves adiabatically with respect to internal degrees of freedom once it is in the activated complex. Thus, the distribution function of the transition structure is adiabatically mapped into  $\varphi$  of the free fragment. The crucial step in the adiabatic mapping is the correlation rule between the quantum states of the TS and those of the free fragments.<sup>16,17</sup>

In this article, we apply the SACM theory to the unimolecular decomposition of protonated fluorobenzene, attempt to estimate the energetics of the fragmentation, and analyze the sources for the different KERs. In addition, we present a refined experimental analysis of the unimolecular decay of  $[\text{C}_6\text{H}_5\text{F}\cdot\text{H}^+]$ . In combining these approaches, several mechanistic variants can be excluded, while a new, hitherto not considered pathway involving the formation of acyclic  $\text{C}_6\text{H}_5^+$  is proposed.

### Theoretical Approach

The SACM calculations for the KER associated with unimolecular HF loss from metastable  $[\text{C}_6\text{H}_5\text{F}\cdot\text{H}^+]$  were performed as described below; full details of adiabatic mapping for a model for fission of a diatomic from a polyatomic molecule are given in Appendix I. All energetics and rotational and vibrational constants of  $[\text{C}_6\text{H}_5\text{F}\cdot\text{H}^+]$  were taken from ab initio calculations performed at the B3LYP/6-31G\*\* level of theory (Appendix II), which compare reasonably well with the previously reported MP2/6-31G\*/HF-6-31G\* calculations.<sup>11</sup> Additional frequency calculations were performed for the fully deuterated species  $[\text{C}_6\text{D}_5\text{F}\cdot\text{D}^+]$ .

We assume that in the TS the motions of the fragments are composed of a motion along the reaction coordinate and two degenerate bending modes, which become rotations in the free HF molecule. Furthermore, we assume that for the energy levels of the bending modes,  $\varphi$  is given by the distribution function of a doubly degenerate harmonic oscillator with a given vibrational temperature ( $T_v$ ). It is convenient to express  $\varphi$  in terms of two quantum numbers, the radial quantum number  $\nu$  ( $\nu = 0, 1, 2, \text{etc.}$ ) and the vibrational angular momentum number  $\omega$  ( $\omega = 0, \pm 1, \pm 2, \text{etc.}$ ). The distribution function of the TS

( $\varphi^\ddagger$ ) is given by eq 1, where the energy is counted from the zero-point energy level  $E_z = h\nu_b$ . Here,  $\nu_b$  is the bending frequency and  $\lambda = \exp(-h\nu_b/kT_v^\ddagger)$ , where  $T_v^\ddagger$  represents the vibrational temperature of the TS.

$$\varphi^\ddagger(\nu, \omega) = (1 - \lambda)^2 \lambda^{(2\nu + |\omega|)} \quad (1)$$

Thus, the distribution function of the free diatomic fragment  $\varphi(j, m)$  is simply  $\varphi^\ddagger(\nu, \omega)$  where the quantum numbers  $\nu$  and  $\omega$  are replaced by the quantum numbers  $j$  and  $m$  of the diatomic species on the basis of the adiabatic correlation, i.e.,  $\nu = j - |m|$  and  $\omega = m$ .<sup>18</sup> Since we are not interested in the projections of  $j$ ,  $\varphi(j)$  is obtained from  $\varphi(j, m)$  by summation over all possible  $m$  with  $-j \leq m \leq j$  expressed in eq 2.

$$\varphi(j) = \sum \varphi^\ddagger(j - |m|, m) = (1 - \lambda)[2\lambda^j - (1 + \lambda)\lambda^{2j}] \quad (2)$$

When the diatomic fragment recedes, the average KER is given by eq 3.

$$\text{KER} = E_a + \Delta E_z + \langle E_v \rangle + E_{\text{rc}} - \langle E_r \rangle \quad (3)$$

Here,  $E_a$  represents the height of the activation barrier with respect to the final dissociation products.  $\Delta E_z$  is the zero-point energy difference between the TS and the products.  $\langle E_v \rangle$  is the average vibrational energy of the bending modes.  $E_{\text{rc}}$  is the energy in the reaction coordinate and  $\langle E_r \rangle$  is the average rotational energy of the fragments. The latter quantity is calculated from  $\varphi(j)$  and the rotational constants  $B$  of the fragments using eq 4 and can be calculated analytically (Appendix I).

$$\langle E_r \rangle = \sum_{j=0}^{\infty} B j(j+1) \varphi(j) \quad (4)$$

In the calculation of the KER, the quantity  $\langle \Delta E_v \rangle$  is subtracted from the sum of energies, because it is not available as translational energy. For experiments in sector mass spectrometers as described below, the translational energy of the incident ion beam is large in the direction of flight (here 8 keV). Since the orientation of the ions in the beam is isotropic, the KER leads to either an increase or decrease of the measured kinetic energy of the fragment ions.

The available ab initio data is used in conjunction with RRKM theory<sup>19</sup> to calculate the energy-dependent unimolecular rate coefficients for the dissociation via various channels. Thus, a combination of RRKM and SACM formalisms allows to predict rate coefficients of unimolecular reactions and the associated KERs. The rate coefficients are used in turn to estimate the internal energies of TS **5** and **6**. The latter determine the vibrational temperatures that are used to calculate  $\lambda$  in eq 1 and  $\langle E_v \rangle$  in eq 3; more details are given in Appendix I.

### Experimental Methods

In addition to the results reported previously,<sup>2,6-11</sup> further experiments concerning the unimolecular dissociation of  $[\text{C}_6\text{H}_5\text{F}\cdot\text{H}^+]$  were performed using a modified VG ZAB/HF/AMD 604 four-sector mass spectrometer of BEBE configuration (B stands for magnetic and E for electric sector) which has been described elsewhere.<sup>20-22</sup> In brief,  $[\text{C}_6\text{H}_5\text{F}\cdot\text{H}^+]$  was generated by chemical ionization (CI) of fluorobenzene with hydrogen as reagent gas. Similarly,  $[\text{C}_6\text{H}_5\text{F}\cdot\text{D}^+]$  was prepared using deuterium as CI gas, and  $[\text{C}_6\text{D}_5\text{F}\cdot\text{D}^+]$  was made from  $[\text{D}_5]$ -fluorobenzene and deuterium. The notation  $[\text{C}_6\text{H}_5\text{F}\cdot\text{H}^+]$  etc. is used throughout and shall not represent a certain structure but only indicates the origin

of H and/or D atoms. Other approaches to  $[C_6H_5F\cdot H^+]$  ions were (i) chemical ionization of benzene and 2,4-hexadiene with  $NF_3$  as reagent gas. (ii) electron ionization of various fluorocarbons, i.e., 3-fluoro-cyclohexene, 1-fluoro-hexa-2,4-diene, 6-fluoro-hexa-1,3-diene, 1,1,1-trifluoro hexan-2-ol, and 1,1,1-trifluoro octan-2-ol. The ions of interest were accelerated to 8 keV kinetic energy and mass selected using magnetic and electric sectors. The unimolecular HF losses from  $[C_6H_5F\cdot H^+]$  were examined in all possible field-free regions of the mass spectrometer at energy resolutions between 1500 and 8000 (i.e., 1–6 eV half width of the parent ion beam) by the following methods:<sup>23,24</sup> (i) direct analysis of the daughter ions formed in the field-free region between the ion source and the first magnet by means of a linked B(1)<sup>2</sup>/E(1) scan; (ii) mass selection of  $[C_6H_5F\cdot H^+]$  with B(1) and recording the fragmentation occurring between B(1) and E(1) by scanning E(1); (iii) mass selection using B(1)/E(1) while monitoring the unimolecular decay between E(1) and B(2) via a linked B(2)<sup>2</sup>/E(2) scan; and (iv) mass-selection of the parent ion with B(1)/E(1)/B(2) and analysis of the fragmentation processes using E(2). In all of these experiments, unimolecular loss of HF from  $[C_6H_5F\cdot H^+]$  gave rise to composite peaks. Except for  $CH_4$  and  $HCl$  as reagent gases (see below), the peak shapes obtained as such were indistinguishable within the experimental uncertainty, regardless of the precursors or the field-free regions used. Hence, the composite nature of the peak shape associated with unimolecular dehydrofluorination is an intrinsic feature of metastable  $[C_6H_5F\cdot H^+]$  and not a remnant of instrumental artifacts.<sup>24</sup> Note that unimolecular loss of  $H^+$  from  $[C_6H_5F\cdot H^+]$  (or  $D^+$  from labeled ions), is negligible if the parent ions are mass selected by double focusing and <sup>13</sup>C contributions of the molecular ion of fluorobenzene are taken into account. All spectra were accumulated and processed online with the AMD/Intectra data system. Five to fifty scans were averaged to improve the signal-to-noise ratio.

For data analysis, the daughter ion profiles have been corrected first for peak asymmetries. In the next step the resulting symmetrized peak vector has been transformed by a complex Fourier transformation. Symmetrically to the middle of the transformation product vector representing the frequency components of the peak, its elements have been successively set to zero. This process was stopped before the first and last vector elements together were involved. Each resulting truncated frequency domain vector then has been inverse complex Fourier transformed and for the resulting disturbed (smoothed) peak vector its information entropy calculated according to the formula

$$\text{information entropy } (v) = \frac{-1}{\ln(2)} \left[ \sum_{i=1}^n \left[ \ln \left[ \frac{v_i}{\sum_{i=1}^n v_i} \right] \left[ \frac{v_i}{\sum_{i=1}^n v_i} \right] \right] \right]$$

Those smoothed peaks have been chosen where the information entropy reached a minimum or a flat plateau at the bottom. Correction for the parent ion width was not necessary for the broad and the medium components of the KER. The resulting peak shapes were analyzed to yield the kinetic energy release distribution (KERD)<sup>15</sup> associated with the unimolecular dehydrofluorination of  $[C_6H_5F\cdot H^+]$ .

A few additional experiments were performed with a CMS 47X Fourier transform ion cyclotron resonance (ICR) mass spectrometer equipped with a 7 T magnet.<sup>25,26</sup> These experiments followed well-established routines of ICR protocols,<sup>25–28</sup> and hence we refrain from an explicit description of the details. In

essence,  $C_6H_5^+$  ions were made by the methods described below, mass selected, thermalized with pulsed-in argon,<sup>29</sup> again mass selected, and reacted with iodobenzene present in the analyzer cell. CMS 47X users should, however, pay attention to footnote 25 in ref 27.

## Results

In the following, we present a detailed discussion of the unimolecular decay of  $[C_6H_5F\cdot H^+]$  when produced via chemical ionization (CI) of fluorobenzene with molecular hydrogen as reagent gas. As reported previously,<sup>11</sup> only the medium and the broad components of the KER are observed experimentally when  $H_2$  is used as a CI gas. The absence of the narrow component can be attributed to the fact that formation of metastable **7** occurs only<sup>5,11</sup> if the proton affinity (PA)<sup>30</sup> of the reagent gas is just a bit lower than that of the F atom in fluorobenzene (PA(F)<sup>11</sup> = 148 kcal/mol), e.g., for the CI gases methane (PA( $CH_4$ ) = 130 kcal/mol) and hydrogen chloride (PA(HCl) = 133 kcal/mol). Protonation with hydrogen (PA( $H_2$ ) = 101 kcal/mol) is too exothermic to yield long-lived **7**; reagents with larger PAs (e.g., water, isobutene, or ammonia) cannot yield metastable **7**.

**Unimolecular Decay of Metastable  $[C_6H_5F\cdot H^+]$ .** Protonation of arenes may be subject to large temperature effects.<sup>5,7</sup> In the instrument used here, temperature effects cannot be studied adequately. Instead, we attempted to alter the internal energy content of metastable  $[C_6H_5F\cdot H^+]$  by varying the pressure of hydrogen which served as CI reagent gas. Upon increasing pressure in the ion source, a weak but distinguishable increase of the medium component of the KER relative to the broad one is observed. Since increasing source pressure generally decreases the ions' internal energies, this observation qualitatively suggests that the medium component of the KER is the more favored the lower the internal energy content. However, owing to the overlap of these two components of the KER and the ill-defined measurement of the actual pressure in the ion source, it is difficult to quantify this effect.

Another attempt to influence the ratio of the two components of the KER was made by varying ion lifetimes, i.e., monitoring unimolecular decay of metastable  $[C_6H_5F\cdot H^+]$  in different field-free regions of the instrument (see Experimental Section). However, the peak shapes obtained this way are indistinguishable from each other, although the ion lifetimes sampled in these experiments range from ca. 1  $\mu s$  in the B(1)<sup>2</sup>/E(1) scan to about 50  $\mu s$  in the E(2) scan.

In addition, we examined the unimolecular loss of HF from  $[C_6H_5F\cdot H^+]$  generated from different precursors. Isobaric interferences notwithstanding, unimolecular losses of molecular hydrogen and hydrogen fluoride are observed almost exclusively. However, the intensity ratio  $I(H_2)/I(HF)$  of these fragmentation channels determined by B(2) scans for B(1)/E(1) mass-selected  $[C_6H_5F\cdot H^+]$  depends on the precursors used. Under similar conditions of ionization and focusing, CI of fluorobenzene with  $H_2$  yields  $I(H_2)/I(HF) \approx 1:10$ , while CI of benzene with  $NF_3$  gives  $I(H_2)/I(HF) \approx 1:2$ , and CI of 2,4-hexadiene with  $NF_3$  gives  $I(H_2)/I(HF) \approx 2:1$ . Nevertheless, B(2)<sup>2</sup>/E(2) linked scans of the HF losses gave the same type of composite peaks for all three precursor mixtures within experimental error. Similarly, identical peak shapes for HF losses were obtained for  $[C_6H_5F\cdot H^+]$  ions made by ionization of several other fluorocarbons (see experimental methods) as well as by protonation of fluorobenzene with other reagent gases. Exceptions are those reagents which closely match the proton affinity of the fluorine atom in fluorobenzene (e.g.,  $CH_4$  and  $HCl$ , see

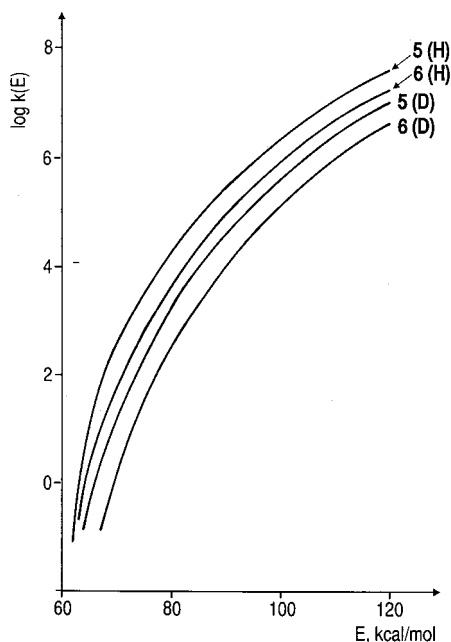


**Figure 3.** RRKM theory unimolecular rate constants  $k(E)$  for the dissociation of protonated (H) and deuterated (D) fluorobenzene via the transition structures **5** and **6** as a function of internal energy relative to the global minimum **1**.

above) and also give rise to the narrow peak due to loss of HF from metastable **7**. Note, however, that even for these reagents the shapes of the medium and broad components are more or less superimposable on those obtained from the other precursors used to generate  $[\text{C}_6\text{H}_5\text{F}\cdot\text{H}^+]$ .

**Rate Coefficients for the Unimolecular Decomposition of Metastable  $[\text{C}_6\text{H}_5\text{F}\cdot\text{H}^+]$ .** CI mass spectrometry involves relatively high pressures, and some collisional cooling of the ions formed can be achieved.<sup>31,32</sup> However, only those  $[\text{C}_6\text{H}_5\text{F}\cdot\text{H}^+]$  ions are relevant in the present context that decompose in the  $\mu\text{s}$  regime. These represent only a minor fraction of the incident beam (ca. 1%) which is per se not thermal.<sup>14</sup> Thermochemical considerations imply that a significant amount of excess internal energy is deposited in  $[\text{C}_6\text{H}_5\text{F}\cdot\text{H}^+]$  when formed with hydrogen as CI gas. For example, paraprotonation of fluorobenzene by  $\text{H}_3^+$  has a reaction exothermicity of  $\Delta_r H = -80$  kcal/mol.<sup>5,11,33</sup> Moreover, chemical ionization in a conventional ion source may involve protonation not only by the predominating Brønsted acid (e.g.,  $\text{H}_3^+$ ) but also by other species that are present as well (e.g.,  $\text{H}_2^+$ ),<sup>34</sup> giving rise to even more energetic protonation events.

To evaluate the rate coefficient of the unimolecular decay of metastable  $[\text{C}_6\text{H}_5\text{F}\cdot\text{H}^+]$ , we calibrated the time scale of the field-free region between B(1) and E(1) by using the previously determined rate coefficient of  $5.3 \times 10^4 \text{ s}^{-1}$  for the unimolecular dehydration of the metastable ethyl acetate cation radical.<sup>35</sup> Considering the size of the KER associated with unimolecular dehydrofluorination of  $[\text{C}_6\text{H}_5\text{F}\cdot\text{H}^+]$ , instrumental discrimination effects were also considered.<sup>36</sup> The average of several measurements is  $k(E) = 5 \pm 3 \times 10^4 \text{ s}^{-1}$  for the unimolecular dehydrofluorination of  $[\text{C}_6\text{H}_5\text{F}\cdot\text{H}^+]$ . This value must be regarded as a rough estimate because the energy distribution in the incident beam is unknown. That is to say, not all  $[\text{C}_6\text{H}_5\text{F}\cdot\text{H}^+]$  ions contain enough energy to undergo fragmentation, and the energy distribution is likely to deviate from Boltzmann behavior.<sup>14</sup> Furthermore, unimolecular dehydrogenation competes with the reaction of interest.<sup>5,6</sup> Thus, the rate coefficient is probably

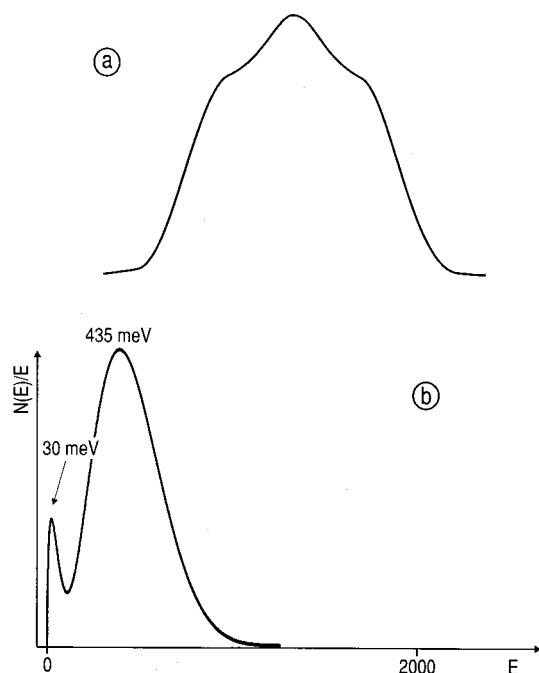


**Figure 4.** (a) Peak shape for the unimolecular loss of HF from  $[\text{C}_6\text{H}_5\text{F}\cdot\text{H}^+]$  in the field-free region preceding  $E(1)$ ; chemical ionization of fluorobenzene with hydrogen. (b) Kinetic energy release distribution (KERD) of the peak shown in Figure 4a.

larger, and in the following analysis, we use  $k(E) = 1 \times 10^5 \text{ s}^{-1}$  and  $3 \times 10^5 \text{ s}^{-1}$  as a rough compromise.

**Internal Energy of Metastable  $[\text{C}_6\text{H}_5\text{F}\cdot\text{H}^+]$ .** The exact internal energy content  $E$  of the metastable ions which decompose in the  $\mu\text{s}$  time scale is uncertain in most mass-spectrometry experiments.<sup>14</sup> To estimate  $E$ , we have used the ab initio data (Appendix II) to calculate the energy-dependent RRKM theory unimolecular rate coefficients,  $k(E)$  for fragmentation of metastable  $[\text{C}_6\text{H}_5\text{F}\cdot\text{H}^+]$  (represented by structure **1**) via **5** and **6** (Figure 3).

Figure 3 has two important implications as to the dissociation of  $[\text{C}_6\text{H}_5\text{F}\cdot\text{H}^+]$ . (i) For values of  $k(E)$  in the order of  $10^5 \text{ s}^{-1}$ , the corresponding internal energies of  $[\text{C}_6\text{H}_5\text{F}\cdot\text{H}^+]$  relative to the global minimum **1** ( $E_{\text{rel}} = 0$  kcal/mol) are about 90 kcal/mol<sup>37</sup> for dissociating via **5** and **6**. This internal energy significantly exceeds the associated barrier heights, i.e., the energy difference between both TSs is small compared to the overall excess energy. (ii) Irrespective of the precise amount of internal energy of metastable  $[\text{C}_6\text{H}_5\text{F}\cdot\text{H}^+]$ , the rate coefficients for dissociation via **5** and **6** are of the same magnitude at internal energies of about 90 kcal/mol. Hence, the intensities of both channels are expected to be of the same order of magnitude, e.g.,  $k(5)/k(6) \approx 2.9$  and  $k(5-D)/k(6-D) \approx 4.1$  at 90 kcal/mol. At this energy, the *intermolecular* kinetic isotope effects amount to  $k(5)/k(5-D) \approx 7.1$  and  $k(6)/k(6-D) \approx 10.0$ . Not surprisingly,<sup>14</sup> the *intramolecular* isotope effects associated with losses of HF and DF from  $[\text{C}_6\text{H}_5\text{F}\cdot\text{D}^+]$  and  $[\text{C}_6\text{D}_5\text{F}\cdot\text{H}^+]$ , respectively, are considerably lower and have previously been determined as  $k_{\text{HF}}/k_{\text{DF}} \approx 2.5$  for these two isotopologs.<sup>11</sup> Note that the match of the intramolecular isotope effects fully confirms H/D equilibration, thereby establishing the involvement of ring-protonated species in the medium and broad components of the KER.

**Experimentally Measured Components of the Kinetic Energy Release.** Figures 4a and 5a show the unimolecular HF and DF losses from  $[\text{C}_6\text{H}_5\text{F}\cdot\text{H}^+]$  and  $[\text{C}_6\text{D}_5\text{F}\cdot\text{D}^+]$ . A cursory

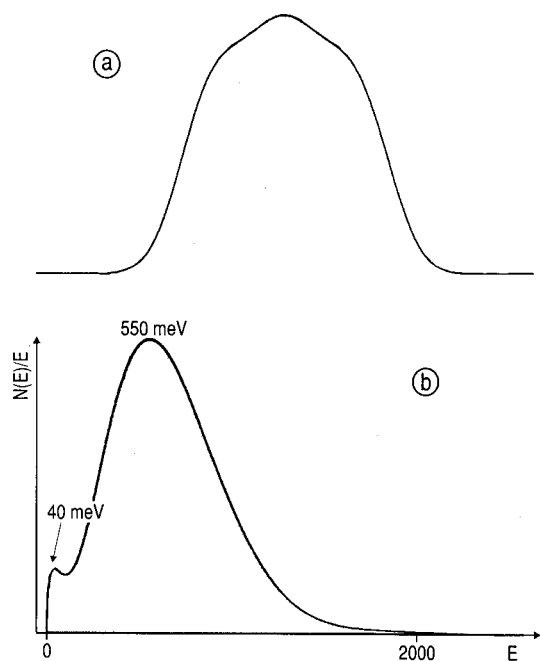


**Figure 5.** (a) Peak shape for the unimolecular loss of DF from  $[\text{C}_6\text{D}_5\text{F}\cdot\text{D}^+]$  in the field-free region preceding  $E(1)$ ; chemical ionization of  $[\text{D}_5]$ -fluorobenzene with deuterium. (b) Kinetic energy release distribution (KERD) of the peak shown in Figure 5a. Note that the experiments for Figures 4 and 5 were performed under the same ion source and focusing conditions.

look reveals already that the relative intensity of the medium component is significantly smaller for the labeled ion.

In the previous crude analysis in terms of  $T_{0.5}$  values,<sup>11</sup> the KERs associated with unimolecular HF losses from  $[\text{C}_6\text{H}_5\text{F}\cdot\text{H}^+]$  were estimated as 16 meV for the medium and 424 meV for the broad component. However, because of the overlap of both components, the  $T_{0.5}$  values are somewhat ill defined. The respective kinetic energy release distribution (KERD)<sup>14</sup> provides a much more sensitive probe. Comparison of the KERDs obtained in several independent experiments for the broad component of the HF loss from  $[\text{C}_6\text{H}_5\text{F}\cdot\text{H}^+]$  leads to the following results: the KER at half-height ( $T_{0.5}$ ) is  $390 \pm 40$  meV, the most probable KER ( $T_{\text{prob}}$ ) is  $435 \pm 40$  meV, and the average KER ( $T_{\text{av}}$ ) is  $600 \pm 50$  meV. While the medium component cannot be analyzed using the simple KERD formalism, the  $T_{\text{prob}}$  value of  $30 \pm 10$  meV is in reasonable agreement with the previous estimate of  $T_{0.5} = 16$  meV for this component.<sup>11</sup> Note that because of the composite peak, the estimate of the KER for the medium component is not very precise and also depends on the actual energy resolution.

A semiquantitative analysis of the KERD curves in Figures 4b and 5b reveals three essential features. (i) Both the medium and the broad components appear at higher energies for the labeled ion, i.e.,  $T_{\text{prob}} = 30 \pm 10$  and  $435 \pm 40$  meV for  $[\text{C}_6\text{H}_5\text{F}\cdot\text{H}^+]$  as compared to  $T_{\text{prob}} = 40 \pm 10$  and  $550 \pm 50$  meV for  $[\text{C}_6\text{D}_5\text{F}\cdot\text{D}^+]$ . This effect is quite common<sup>14</sup> and can be attributed to an increase of the internal energy content upon deuteration as well as the different energy distributions in the fragmentation of the labeled ion. (ii) The abundances of the broad components of the fully deuterated and the unlabeled ion are similar, while that of the medium component is subject to a kinetic isotope effect which leads to a significant decrease of its abundance for  $[\text{C}_6\text{D}_5\text{F}\cdot\text{D}^+]$ . (iii) The (integrated) intensities of the medium and the broad components differ by about an order of magnitude for the unlabeled and the labeled ion. Thus, the ratio between the broad and the medium component is ca. 10:1 for  $[\text{C}_6\text{H}_5\text{F}\cdot\text{H}^+]$

**TABLE 1: Excess Energy  $E$  and Vibrational Temperature  $T_v$  of the Product Complex **7** Dissociating into Singlet (S) and Triplet (T) Phenyl Cation and HF via the Transition Structures **5** and **6**, Respectively, and the Resulting Energies in Individual Transition Modes  $\langle E_{v,i} \rangle$  and Their Sum  $\langle E_v \rangle$**

structure	$E$ kcal/mol	$T_v$ K	$\langle E_{v,i} \rangle$ kcal/mol frequency, $\text{cm}^{-1}$				$\langle E_v \rangle$ kcal/mol
			165	169	247	714	
Protonated							
$k(E) = 1 \times 10^5 \text{ s}^{-1}$							
5S	29.3	998	1.8	1.7	1.6	1.1	6.2
5T	9.8	567	0.9	0.9	0.8	0.4	3.0
6S	33.8	1086	1.9	1.9	1.8	1.3	7.0
6T	14.2	626	1.0	1.0	0.9	0.5	3.4
$k(E) = 3 \times 10^5 \text{ s}^{-1}$							
5S	34.3	1074	1.9	1.9	1.8	1.3	6.9
5T	14.8	662	1.1	1.1	1.0	0.6	3.7
6S	38.3	1151	2.0	2.0	1.9	1.4	7.4
6T	18.7	752	1.3	1.3	1.1	0.7	4.4
structure	$E$ kcal/mol	$T_v$ K	$\langle E_{v,i} \rangle$ kcal/mol frequency, $\text{cm}^{-1}$				$\langle E_v \rangle$ kcal/mol
			121	156	234	554	
Deuterated							
$k(E) = 1 \times 10^5 \text{ s}^{-1}$							
5S	36.3	1041	1.9	1.8	1.7	1.4	6.9
5T	17.0	662	1.2	1.1	1.0	0.7	3.9
6S	41.8	1140	2.1	2.0	1.9	1.6	7.6
6T	22.5	778	1.4	1.3	1.2	0.9	4.8
$k(E) = 3 \times 10^5 \text{ s}^{-1}$							
5S	41.3	1132	2.1	2.0	1.9	1.5	7.6
5T	22.0	767	1.3	1.3	1.2	0.9	4.7
6S	46.8	1229	2.3	2.2	2.1	1.7	8.3
6T	27.5	876	1.6	1.5	1.4	1.1	5.6

$\text{H}^+$  and ca. 18:1 for  $[\text{C}_6\text{D}_5\text{F}\cdot\text{D}^+]$ . Note that these ratios have to be regarded as lower limits as a result of instrumental discrimination of the broad component by the considerable KER.<sup>36</sup> The same conclusion can be derived from a linked B(2)/E(2) scan analysis of the competing HF and DF losses in the unimolecular decay of metastable  $[\text{C}_6\text{H}_5\text{F}\cdot\text{D}^+]$  generated by deuteration of fluorobenzene. The medium component is hardly observed in the DF loss channel but is clearly discernible for the HF loss, and  $T_{\text{prob}}$  of the broad component is significantly larger for loss of DF ( $565 \pm 60$  meV) than for loss of HF ( $435 \pm 50$  meV). Thus, we conclude that as far as the ratio of the two components of the KER is concerned, intra- and intermolecular kinetic isotope effects are similar such that the qualitative comparison of  $[\text{C}_6\text{H}_5\text{F}\cdot\text{H}^+]$  and  $[\text{C}_6\text{D}_5\text{F}\cdot\text{D}^+]$  is justified.<sup>14,38</sup>

**Calculation of the Kinetic Energy Releases.** The reaction coordinates and the four transition modes of the protonated and deuterated fluorobenzenes were derived from ab initio calculations. Further, the C–F stretching vibration can be correlated to the reaction coordinate. The four relevant transition modes in **7** are (i) free or hindered rotation of the HF group ( $165 \text{ cm}^{-1}$ ), (ii) HF bending combined with ring puckering ( $169 \text{ cm}^{-1}$ ), (iii) HF bending relative to the arene ring ( $247 \text{ cm}^{-1}$ ), and (iv) the H bend in the HFC group ( $714 \text{ cm}^{-1}$ ). The corresponding frequencies in the deuterated species are 121, 156, 234, and  $554 \text{ cm}^{-1}$ . The energy contents of the transition modes at various temperatures as determined by RRKM theory calculations (see above) are given in Table 1. The energy in the two low-lying modes approaches the classical value of  $kT_v$ , while the energy content of the highest transition modes is well below  $kT_v$ .

The KERs associated with the dissociation of **7** formed via **5** or **6**, respectively, into HF and singlet (S) and triplet (T) phenylum cations  $\text{C}_6\text{H}_5^+$  are given in Table 2. It is apparent that the transition structures **5** and **6** both lead to KERs  $> 300$  meV. This result rules out the previous<sup>11</sup> hypothesis that the

**TABLE 2: Vibrational Temperatures  $T_v$ , Energies (kcal/mol) in the Transition Modes  $\langle E_v \rangle$ , Zero-Point Energy Differences  $E_{zp}$ , Energies in the Reaction Coordinate  $E_{rc}$ , Average Rotational Energies  $\langle E_r \rangle$ , and the Kinetic Energy Releases (KER) for the Decay of Protonated Fluorobenzene via the Transition Structures **5** and **6** to Yield Singlet (S) or Triplet (T) Phenylum, Respectively**

	$T_v$ (K)	$\langle E_v \rangle$	$\Delta E_{zp}$	$E_{rc}$	$\langle E_r \rangle$	KER (meV)	
						no rotation	with rotation
Protonated							
$k(E) = 1 \times 10^5 \text{ s}^{-1}$							
5S	998	6.2	2.7	2.0	3.7	473	312
5T	567	3.0	2.2	1.2	1.2	278	226
6S	1086	7.0	2.7	2.2	4.4	516	327
6T	626	3.4	2.2	1.3	1.4	230	236
$k(E) = 3 \times 10^5 \text{ s}^{-1}$							
5S	1074	6.9	2.7	2.2	4.3		324
5T	662	3.7	2.2	1.3	1.6		243
6S	1151	7.4	2.7	2.3	4.9		327
6T	752	4.4	2.2	1.5	2.1		260
Protonated (Free Rotor)							
$k(E) = 1 \times 10^5 \text{ s}^{-1}$							
5S	998	6.2	2.7	2.0	4.7	399	269
5T	567	3.0	2.2	1.2	1.9	239	194
6S	1086	7.0	2.7	2.2	5.4	434	281
6T	626	3.4	2.2	1.3	2.2	256	201
$k(E) = 3 \times 10^5 \text{ s}^{-1}$							
5S	1074	6.9	2.7	2.2	5.3		279
5T	662	3.7	2.2	1.3	2.5		207
6S	1151	7.4	2.7	2.3	6.0		281
6T	752	4.4	2.2	1.5	3.0		221
Deuterated (Free Rotor)							
$k(E) = 1 \times 10^5 \text{ s}^{-1}$							
5S	1041	6.6	2.3	2.1	2.6	490	380
5T	662	3.9	2.0	1.4	1.0	316	273
6S	1140	7.6	2.3	2.3	3.0	529	397
6T	778	4.4	2.0	1.6	1.4	364	303
$k(E) = 3 \times 10^5 \text{ s}^{-1}$							
5S	1132	7.6	2.3	2.3	3.0		395
5T	767	4.7	2.0	1.5	1.4		297
6S	1229	8.3	2.3	2.5	3.6		413
6T	876	5.6	2.0	1.8	1.8		326

experimentally observed medium component ( $\sim 30$  meV) emanates from dissociation via one TS and the broad component ( $\sim 435$  meV) from the other TS. Instead, as long as the ions behave statistically, both TSs contribute to the broad feature. The medium component also cannot be due to the production of triplet phenylum, because the KERs emanating from triplet  $C_6H_5^+$ , though smaller than for the singlet, are still  $> 190$  meV.

The theoretical analysis properly describes the main experimental features of the broad component of the KER. Thus, the deuterated ion gives a larger KER than the protonated one, and both are in the order of several hundreds of meV. On the whole, the calculated KERs are somewhat smaller than the experimental values, and apparently the exclusion of product rotation results in a better agreement with experiment. An exit-channel barrier between **7** and the products could explain the remaining discrepancy. However, careful ab initio studies of the reaction coordinate showed no such barrier. Therefore, explanations may rest in other factors such as the breadth of the energy distribution in the ions, which was not considered by theory, or, more simply, in the experimental uncertainty of the absolute KER measurement.<sup>39,40</sup>

### Possible Mechanisms for the Unimolecular Dissociation of Protonated Fluorobenzene

Before analyzing the components of the KER associated with loss of HF from  $[C_6H_5F \cdot H^+]$ , let us briefly outline the boundary

conditions which must be met by possible scenarios. (i) The narrow component is due to direct protonation at fluorine<sup>2,11</sup> and will not be discussed any further. The other two components emanate from ring protonation. (ii) Unimolecular dissociation of ring-protonated fluorobenzene in the  $\mu\text{s}$  regime requires an excess energy of about 90 kcal/mol relative to **1**. (iii) The calculated KERs for the dissociations via **5** and **6** are in accord with the broad component but clearly cannot account for the medium one. (iv) The contribution of the medium component is subject to a significantly larger H/D kinetic isotope effect than the broad one. (v) Finally, in a more complete mechanistic picture, also the observed competition of unimolecular  $H_2$  and HF losses as well as the slight pressure effect on the peak shapes must be explained.

Quite clearly, the broad component can safely be attributed to (statistical) dissociations via **5** and **6** in that both involve ring-protonated species, the predicted rate coefficients are similar, and the measured and calculated KERs agree reasonably well. It is the origin of the medium component that remains unclear. However, as this component also involves ring-protonation, it is not the reactant side that is in question but the particular outcome on the product side, which gives rise to the medium component of the KER.

**Dynamic Behavior—The Old Explanation.** Previously,<sup>11</sup> the two components of the KER were attributed to different degrees of energy dissipation in the exit channels starting from **5** or **6**. In fact, the present analysis reveals that **7**, which is common to both TS, is “hot”, i.e., it possesses a large amount of excess energy (ca. 60 kcal/mol) when formed from metastable  $[C_6H_5F \cdot H^+]$ . RRKM theory estimates an upper limit of only about 20 fs for the lifetime of hot **7**. The reaction may therefore proceed directly from **5** or **6** to the products without residing in structure **7**. That is to say, full energy randomization may not take place once **7** is formed via **5** or **6**, thus preserving some memory of the preceding TS. Accordingly, dynamic behavior as the source of the two components of the KER cannot be ruled out using statistical arguments.

Nevertheless, the experimentally determined ratio of the two components disfavors competing dissociations via **5** and **6** as a source for the different KERs. Even though excited **7** may not be treated statistically, the reactants **1–4** as well as **5** and **6** certainly can. The satisfactory agreement between the measured and calculated KERs of the broad component further substantiates this point of view. Accordingly, competing decays via **5** and **6** should coincide with the ca. 3:1 ratio predicted by RRKM theory. Experimentally, however, the broad component prevails by an order of magnitude. In addition, RRKM theory predicts minor intermolecular kinetic isotope effects, i.e.,  $k(\mathbf{5})/k(\mathbf{6}) \approx 2.9$  and  $k(\mathbf{5}-D)/k(\mathbf{6}-D) \approx 4.1$ , whereas the measured ratios of the two components for  $[C_6H_5F \cdot H^+]$  and  $[C_6D_5F \cdot D^+]$  are significantly larger, i.e., 10:1 vs 18:1. Consequently, even though passages via **5** and **6** are indeed expected to compete in the dissociation of metastable  $[C_6H_5F \cdot H^+]$ , this competition cannot be considered as a source of the different KERs. As a note of caution, we should add, however, that the accuracy of the rate constants determined via the RRKM approach is limited. Even though we consider the relative rate constants for passages via **5** and **6**, uncertainties in the transition-state parameters might alter the ratio of the rate constants. For the time being, however, we have no appropriate means available to more adequately describe the polyatomic system under study.

**Vibrational Excitation of Hydrogen Fluoride.** Another explanation for the medium component involves the formation of vibrationally excited HF in addition to the ground-state

product. In fact, the first vibrational level of hydrogen fluoride ( $4139\text{ cm}^{-1} \cong 510\text{ meV}$ ) roughly fits the energy difference between the two components of the KER. The probability ( $P$ ) of finding HF in  $\nu = 1$  is given by the Boltzmann expression (eq 5).

$$P_{(\nu=1)} = \exp(-h\nu_{\text{HF}}/kT_{\nu}) / (1 - \exp(-h\nu_{\text{HF}}/kT_{\nu})) \quad (5)$$

For the vibrational temperatures involved, the probability of the formation of vibrationally excited HF is therefore in the order of 2%, and if a distribution of internal energies is assumed,  $P_{(\nu=1)}$  may even be larger. Formation of HF ( $\nu = 1$ ) would provide a simple explanation for the magnitude of the KER difference as well as the relative intensities of the two components. The broad component could be assigned to internally excited phenyl cation and HF ( $\nu = 0$ ). In turn, excitation to HF ( $\nu = 1$ ) leaves the phenyl fragment "cold", giving rise to the medium component. The latter process is less probable and therefore of lower intensity.

Nevertheless, the data of the fully deuterated ion [ $\text{C}_6\text{D}_5\text{F}\cdot\text{D}^+$ ] excludes this option. Considering the lower vibrational frequency of DF ( $2998\text{ cm}^{-1} \cong 370\text{ meV}$ ), the medium component should exhibit a considerably larger KER than for HF loss, i.e., about 170 meV for the deuterated ion instead of a measured value of  $40 \pm 10\text{ meV}$  for the medium component. Further, loss of DF ( $\nu = 1$ ) is expected to gain in intensity because excitation of DF is more facile than of HF. Experimentally, the opposite effect is observed. The intensity of the medium component is lower for the deuterated ion, and the slight increase of the corresponding KER upon deuteration<sup>14</sup> is much smaller than the energy difference of  $\nu_{\text{HF}}$  and  $\nu_{\text{DF}}$ . Thus, while vibrational excitation of the leaving HF molecule appears as a straightforward scenario, it cannot account for the bimodal KER observed experimentally.

**Electronic Excitation.** In the previous interpretation of the KER features,<sup>11</sup> electronic excitation has been proposed as a feasible product channel in that a triplet state of the phenyl cation may be formed because the singlet–triplet gap for  $\text{C}_6\text{H}_5^+$  was anticipated to be small (ca. 5 kcal/mol).<sup>41–43</sup> Improved theoretical calculations have meanwhile demonstrated that the singlet–triplet gap for phenyl cation is almost 1 eV.<sup>44,45</sup> In conjunction with the considerable energy content of the metastable ions, curve crossing to the triplet surface may therefore appear as a possible option in the unimolecular dissociation of [ $\text{C}_6\text{H}_5\text{F}\cdot\text{H}^+$ ].<sup>46</sup> Moreover, the considerable spin–orbit coupling constant of atomic fluorine may facilitate intersystem crossing. Formation of triplet phenyl cation would imply that a significant fraction of the excess energy gained upon dissociation is stored as potential energy of the excited product state and is therefore not available for the KER. Indeed, the calculated KERs for formation of triplet  $\text{C}_6\text{H}_5^+$  concomitant with neutral HF are considerably lower than those for the singlet products (Table 2) but still fall in a range of 190–260 meV, which does not fit either of the experimentally measured components of the KER. Further, the pronounced isotope effect on the two components of the KER observed experimentally is difficult to explain in this model because spin interconversion presumably involves the heavy atoms (C and F) rather than H or D. Hence, formation of triplet species may occur to a minor extent, but whether or not this happens, it does not provide a rationale for the bimodal behavior of the KER.

**Isomerization of the Reactant and/or Formation of Different  $\text{C}_6\text{H}_5^+$  Isomers.** Following the arguments raised above, we are left with the alternative that there exists other pathways for loss of HF from [ $\text{C}_6\text{H}_5\text{F}\cdot\text{H}^+$ ]. More precisely, the previous

exclusion of ring-opened  $\text{C}_6\text{H}_5^+$  products is in question.<sup>11</sup> Ab initio calculations indicate that within the energy content of metastable [ $\text{C}_6\text{H}_5\text{F}\cdot\text{H}^+$ ] fluorine migrations, including insertion in the C–C backbone and rearrangement to the fluorepinium structure, are feasible.<sup>11,47,48</sup> These processes may also involve formation of acyclic isomers. Ring-opening would lead to products other than phenylum and is presumably less exothermic.<sup>12</sup> Consequently, as with the triplet channel (see above), part of the excess energy is stored as potential energy such that less energy is available as translation. The KER would therefore decrease accordingly.

Experimentally, we made several attempts to examine unimolecular dehydrofluorination of [ $\text{C}_6\text{H}_5\text{F}\cdot\text{H}^+$ ] generated from acyclic precursors as possible routes to acyclic  $\text{C}_6\text{H}_5^+$ . As mentioned above, the resulting peak shapes associated with HF losses from the corresponding [ $\text{C}_6\text{H}_5\text{F}\cdot\text{H}^+$ ] cations were similar to those reported in Figure 4a. The vast amount of possible acyclic isomers (and cyclic systems other than six-membered rings) does not, however, allow to exclude the option that a minor fraction of the incident [ $\text{C}_6\text{H}_5\text{F}\cdot\text{H}^+$ ] ions decompose via ring-opening. In fact, Eyler and Campana<sup>12</sup> have reported that dissociative ionization of benzene derivatives may lead to mixtures of phenyl cation with some acyclic isomers. Although it has been demonstrated<sup>34</sup> that chemical ionization of halobenzenes with Brønsted acids preferentially leads to phenyl cation, formation of acyclic isomers as minor side products could not be excluded. Conceptually, there exists an option to probe this hypothesis, because it implies that the different components of the KER consist of isomeric  $\text{C}_6\text{H}_5^+$  ions, which may be distinguished by means of MS/MS experiments. For example, Eyler and Campana<sup>12</sup> have provided criteria for the distinction of acyclic  $\text{C}_6\text{H}_5^+$  ions from the phenylum by means of charge-stripping mass spectrometry.

Unfortunately, the energy resolution required for a reasonable separation of the two components of the KER associated with unimolecular HF loss from [ $\text{C}_6\text{H}_5\text{F}\cdot\text{H}^+$ ] is associated with a considerable decrease in ion transmission. Thus, except collisional activation (CA), any further attempts to structurally characterize the  $\text{C}_6\text{H}_5^+$  ions of these components by subsequent collision experiments were impossible. Moreover, the MI/CA spectra of the energy-resolved components of the  $\text{C}_6\text{H}_5^+$  ions formed upon dehydrofluorination of metastable [ $\text{C}_6\text{H}_5\text{F}\cdot\text{H}^+$ ] ions were indistinguishable within experimental error. This result is not very conclusive, however, because even at the center of the peak, the broad component prevails (Figure 2) and collisional activation is not a particularly diagnostic probe for  $\text{C}_6\text{H}_5^+$  ion structures.<sup>12</sup>

Owing to these experimental difficulties and the complexity of the [ $\text{C}_6\text{H}_5$ ]<sup>+</sup> potential-energy surface,<sup>12,34</sup> we are left with the option of ring-opening of [ $\text{C}_6\text{H}_5\text{F}\cdot\text{H}^+$ ] as a possible origin for the medium component of the KER. So far we cannot unambiguously deduce this conclusion from either experiment or theory. Nevertheless, three pieces of information lend credit to this hypothesis. (i) The high energy content of metastable [ $\text{C}_6\text{H}_5\text{F}\cdot\text{H}^+$ ] before dissociating into  $\text{C}_6\text{H}_5^+$  and HF renders ring-opening conceivable, in particular, because isomerization of phenyl to acyclic isomers is kinetically favored at high temperatures.<sup>49,50</sup> (ii) Rearrangement of the reactant ion prior to dissociation is likely to involve additional hydrogen migrations, thus providing a simple rationale for the significantly larger kinetic isotope effects of the medium component of the KER as compared to the broad one. (iii) Finally, involvement of acyclic structures in the reactant ion can account for the variations of the ratio of  $\text{H}_2$  and HF losses for metastable

[C<sub>6</sub>H<sub>5</sub>F·H<sup>+</sup>] ions generated from different precursors. Thus, loss of HF can be attributed to a genuine fragmentation of protonated fluorobenzene, while dehydrogenation may involve isomeric species as well. This particular argument is reinforced by the fact that loss of H<sub>2</sub> is completely absent in low-energy collision-induced dissociation (CID) of thermalized protonated fluorobenzene, in which only dehydrofluorination occurs.<sup>6</sup> For the metastable ions, however, H<sub>2</sub> and HF losses compete with each other, and the ratio depends on the precursors used to generate [C<sub>6</sub>H<sub>5</sub>F·H<sup>+</sup>]. These seemingly contradictory results cannot be explained by invoking a single set of interconverting isomers alone, i.e., ring-protonated fluorobenzene, because low-energy CID and metastable ion spectra sample the low-energy exit channels of a given potential-energy surface. Thereby, the complete absence of dehydrogenation upon low-energy CID of thermalized [C<sub>6</sub>H<sub>5</sub>F·H<sup>+</sup>] points toward the presence of isomeric structures other than protonated fluorobenzene in our experiments rather than to differences in the internal energy content.

### ICR Experiments

Summarizing the discussion so far, we are left with an unsatisfying explanation for the origin of the medium component of the KER. While the experimental and theoretical results imply that the broad component can be attributed to dissociation via **5** and **6**, and several explanations for the origin of the medium component of the KER can be ruled out, a definitive assignment of the origin of the medium component has not yet been achieved.

A possible way to resolve the remaining uncertainties would be to perform experiments, which can somehow specifically probe the properties of the C<sub>6</sub>H<sub>5</sub><sup>+</sup> ions formed. While other kinds of collision experiments using sector mass spectrometry are conceivable,<sup>12</sup> these are unlikely to provide unambiguous answers. In fact, even if there would exist some discernible differences between the ions that contribute to the two components of the KER, these differences could either be attributed to different structures or different internal energies. For example, if we assume that the broad component of the KER corresponds to the generation of phenyl cation in its singlet ground state, the medium component contains either electronically excited phenylium and/or other isomers. Accordingly, further experiments using sector mass spectrometry are likely to complicate rather than to solve the present problem.

Therefore, we decided to employ ion cyclotron resonance (ICR) mass spectrometry as an entirely different experimental approach. In ICR mass spectrometry, no distinction of KERs can be made because the cyclotron frequency is primarily a function of mass and is independent of translational energy. If, however, protonation of fluorobenzene with strong Brønsted acids gives rise to isomeric C<sub>6</sub>H<sub>5</sub><sup>+</sup> products, these could possibly be distinguished by means of their subsequent ion/molecule reactions.<sup>34</sup> Because of the complexity of the [C<sub>6</sub>H<sub>5</sub>]<sup>+</sup> surface, let us consider only three different cases: (a) ground-state phenylium ion; (b) excited phenylium ion (or cyclic structures other than phenylium);<sup>51,52</sup> and (c) acyclic C<sub>6</sub>H<sub>5</sub><sup>+</sup> isomers.

Differentiating between these options requires a sensitive probe for further ion/molecule reactions.<sup>53</sup> We have chosen iodobenzene on the basis of the following considerations. Iodobenzene has an ionization energy (IE) of 8.69 eV.<sup>54</sup> Hence, thermalized ground-state phenyl cation cannot undergo charge transfer to yield C<sub>6</sub>H<sub>5</sub>I<sup>+</sup> molecular ion, because the adiabatic IE of phenyl radical (8.32 eV)<sup>55</sup> is too low.<sup>44,45</sup> Electronically, rovibrationally, or translationally excited phenyl cation can undergo charge transfer to form C<sub>6</sub>H<sub>5</sub>I<sup>+</sup>, however. Polycyclic isomers are expected to behave similarly. Conceivably, acyclic

C<sub>6</sub>H<sub>5</sub><sup>+</sup> isomers are likely to experience considerable stabilization of the carbocationic center by adjacent multiple bonds. For example, even IE of propargyl radical (8.67 eV)<sup>54</sup> is slightly lower than that of iodobenzene and substitution should further decrease the IE of acyclic C<sub>6</sub>H<sub>5</sub><sup>+</sup>, e.g., IE(H<sub>3</sub>CCCCH<sub>2</sub>)<sup>54</sup> = 7.97 eV and IE(HCCCCH·CHCH<sub>2</sub>)<sup>54</sup> = 7.88 eV. Hence, charge transfer is not to be expected for the acyclic species. In view of the considerable heats of formation of polyacetylenes, e.g., H<sub>3</sub>-CCCCCCH<sub>3</sub> → C<sub>6</sub>H<sub>6</sub> + 70 kcal/mol, charge transfer with iodobenzene may occur, however, if associated with a rearrangement of the acyclic species to the phenyl structure.<sup>54</sup> Interestingly, the proton affinities (PA) of highly unsaturated hydrocarbons are comparable to the PAs of arenes, e.g.,<sup>30</sup> PA-(HCCCCH) = 176 kcal/mol, PA(H<sub>3</sub>CCCH) = 179 kcal/mol, and PA(H<sub>3</sub>CCCCCH<sub>3</sub>) = 186 kcal/mol versus PA(C<sub>6</sub>H<sub>6</sub>) = 180 kcal/mol, PA(C<sub>6</sub>H<sub>5</sub>F) = 181 kcal/mol, PA(C<sub>6</sub>H<sub>5</sub>Cl) = 180 kcal/mol, and PA(C<sub>6</sub>H<sub>5</sub>Br) = 180 kcal/mol. No data were found for the proton affinity of iodobenzene, but it can safely be assumed to fall in the same margin.<sup>56</sup> Therefore, it appears conceivable that acyclic C<sub>6</sub>H<sub>5</sub><sup>+</sup> isomers inter alia undergo proton transfer with iodobenzene.

As a prerequisite for an application of this kind of analysis to the protonation of fluorobenzene, these suggestions have to be probed experimentally, and next we discuss the three scenarios mentioned above.

**a. Ground-state phenylium ion.** At first, the reactivity of ground-state phenylium C<sub>6</sub>H<sub>5</sub><sup>+</sup> (<sup>1</sup>A<sub>1</sub>) needs to be established. To this end, C<sub>6</sub>H<sub>5</sub><sup>+</sup> was generated by abstraction of iodide from iodobenzene, but instead of using Brønsted acids, we employed Lewis acids for this purpose, i.e., bare Cu<sup>+</sup> and Au<sup>+</sup>. The advantage of using these metal cations with s<sup>0</sup>d<sup>10</sup> ground-state configurations is twofold. The atomic ions have no low-lying excited states, rovibrational cooling is nonexistent, and translational cooling is facile by collision with nonreactive buffer gases.<sup>29</sup> Experimentally,<sup>57,58</sup> Cu<sup>+</sup> and Au<sup>+</sup> were allowed to react with iodobenzene (p ≈ 6 × 10<sup>-9</sup> mbar) for about 5 s. The C<sub>6</sub>H<sub>5</sub><sup>+</sup> formed was mass-selected, thermalized by pulsing-in argon (ca. 2000 collisions), mass-selected again, and then trapped in the presence of iodobenzene. The so-formed C<sub>6</sub>H<sub>5</sub><sup>+</sup> undergoes exclusively C–C coupling to predominately yield C<sub>12</sub>H<sub>10</sub><sup>+</sup> (probably ionized biphenyl) along with ca. 5% C<sub>12</sub>H<sub>9</sub><sup>+</sup> (probably phenylphenylium).<sup>34</sup> Neither charge- nor proton transfers are observed. We assign this behavior as a fingerprint of thermalized ground-state phenylium ion.

**b. Excited Phenylium Ion.** For C<sub>6</sub>H<sub>5</sub><sup>+</sup> generated by dissociative ionization of iodobenzene in the external ion source, C–C coupling also predominates. However, charge transfer is observed as a minor channel (ca. 5%) even at the lowest electron energies used for ionization (ca. 12.5 eV compared to a threshold of ca. 11.5 eV).<sup>35</sup> Similarly, without ion thermalization some charge transfer is observed in the route via C<sub>6</sub>H<sub>5</sub>I and Au<sup>+</sup>. The amount of charge transfer drastically increases, if the electron energy in ionizing iodobenzene is increased and/or the thermalization sequence is omitted. However, proton transfer from C<sub>6</sub>H<sub>5</sub><sup>+</sup> to iodobenzene is not observed to a significant extent. The latter process is indeed not expected to occur for phenylium, even though excited, because the proton affinity of *o*-benzyne as the neutral counterpart is rather large (201 kcal/mol).<sup>30</sup> Consequently, we attribute this behavior to the presence of excited phenylium.

**c. Acyclic C<sub>6</sub>H<sub>5</sub><sup>+</sup> Isomers.** Dissociative ionization of 2,4-hexadiyne yields C<sub>6</sub>H<sub>5</sub><sup>+</sup> which, after thermalization with argon, reacts with iodobenzene via C–C coupling (90%) along with proton transfer (10%) to yield C<sub>6</sub>H<sub>6</sub>I<sup>+</sup>, while charge transfer is negligible (<2%). This is precisely what we would expect when acyclic C<sub>6</sub>H<sub>5</sub><sup>+</sup> species are formed (see above). Thus, we assign



**TABLE 3: Reactivity Pattern of C<sub>6</sub>H<sub>5</sub><sup>+</sup> Cations Formed in Different Ways Using Iodobenzene as a Monitor**

method	assignment <sup>a</sup>	C–C coupling	charge transfer	proton transfer
C <sub>6</sub> H <sub>5</sub> I + M <sup>+</sup> (M = Cu, Au) <sup>b</sup>	ground-state phenylium	++	–	–
electron ionization of C <sub>6</sub> H <sub>5</sub> I <sup>c</sup>	excited phenylium	++	+	–
ionization of 2,4-hexadiyne	acyclic C <sub>6</sub> H <sub>5</sub> <sup>+</sup>	++	–	+
ArH <sup>+</sup> /fluorobenzene	mixture	++	+	+

<sup>a</sup> The assignments refer to the categories defined in the text. “++” stands for the major route, “+” for minor channels, and “–” for the absence of particular pathways. <sup>b</sup> Including thermalization of C<sub>6</sub>H<sub>5</sub><sup>+</sup> by pulsed-in argon. <sup>c</sup> Similar results are obtained when thermalization of C<sub>6</sub>H<sub>5</sub><sup>+</sup> is omitted in the C<sub>6</sub>H<sub>5</sub>I/M<sup>+</sup> couple.

this behavior to the third category. We note in passing that C<sub>6</sub>H<sub>5</sub><sup>+</sup> generated by dissociative electron ionization (70 eV) of benzene undergoes all three reactions, i.e., C–C coupling as well as charge- and proton transfer.<sup>45</sup>

There is, therefore, a fortuitous situation where simple ion/molecule reactions provide a possible means to qualitatively distinguish between the three alternatives defined above. Nevertheless, methods (b) and (c) probably yield mixtures of different C<sub>6</sub>H<sub>5</sub><sup>+</sup> species. Quantitative analysis of the C<sub>6</sub>H<sub>5</sub><sup>+</sup> species is rather difficult, however, because the thermalization sequence as well as reactions with iodobenzene during the thermalization sequence could seriously affect the initial distributions. For example, unimolecular and/or collision-induced intersystem crossing may deplete electronically excited states,<sup>52</sup> and C<sub>6</sub>H<sub>5</sub> exchange with the iodobenzene may alter the nature of the C<sub>6</sub>H<sub>5</sub><sup>+</sup> species under study. In the present context, however, it is completely sufficient that the criteria outlined above differ not only quantitatively but also qualitatively. Thermalized C<sub>6</sub>H<sub>5</sub><sup>+</sup> undergoes exclusive C–C bond coupling, excited phenylium ions also undergo charge transfer, while the putative acyclic C<sub>6</sub>H<sub>5</sub><sup>+</sup> isomers allow for proton transfer as well (Table 3).

Having made this qualitative distinction, application to C<sub>6</sub>H<sub>5</sub><sup>+</sup> formed by dissociative protonation of fluorobenzene seems obvious. For dehydrofluorination of ring-protonated fluorobenzene in an ion/molecule reaction to occur, the net reaction exothermicity must exceed the reaction barriers via **5** and/or **6**. Accordingly, the Brønsted acids must be at least 60 kcal/mol more acidic than **1**. Reasonable yields of C<sub>6</sub>H<sub>5</sub><sup>+</sup> are expected to require even larger exothermicities due to energy transfer to the leaving deprotonated acid as well as the competition of radiative cooling with unimolecular dissociation. In this respect, molecular hydrogen (PA = 101 kcal/mol)<sup>30</sup> seems ideal because it exceeds the proton affinity of fluorobenzene by about 80 kcal/mol. Furthermore, chemical ionization of fluorobenzene with H<sub>2</sub> as reagent gas gives rise to the composite peaks shown in Figures 4a and 5a. It is a matter of irony that our advanced 7 T ICR instrument is not particularly suited for this purpose. Thus, while the high-field magnet provides a large resolving power, ions below *m/z* = 17 amu cannot be handled or detected, simply because their resonance frequencies are too high. As a compromise, we have examined the following sequence. Argon (PA = 88 kcal/mol)<sup>30</sup> was ionized in the external ion source, transferred to the analyzer cell, Ar<sup>+</sup> was mass-selected, and then reacted with a pulsed-in ca. 20:1 mixture of hydrogen and fluorobenzene.<sup>34</sup> After the gas pulse was pumped away (ca. 3 s), the C<sub>6</sub>H<sub>5</sub><sup>+</sup> species thus formed were mass-selected and trapped for 5 s with a 1:10 mixture of iodobenzene and argon. Then, remaining C<sub>6</sub>H<sub>5</sub><sup>+</sup> was mass-selected again, and its reaction with iodobenzene was monitored. Experimentally, we find that C–C coupling prevails for the C<sub>6</sub>H<sub>5</sub><sup>+</sup> species generated this way, but a significant fraction of proton transfer along with a small amount of charge transfer is observed as well. While this result is not directly related to the particular components of the KER for the metastable ions, it clearly demonstrates that protonation of fluorobenzene with strong Brønsted acids such

as ArH<sup>+</sup> can cause the formation of acyclic C<sub>6</sub>H<sub>5</sub><sup>+</sup> species as indicated by the characteristic proton transfer to iodobenzene. Therefore, these ion/molecule reactions strongly support the suggestion that ring-opening to acyclic C<sub>6</sub>H<sub>5</sub><sup>+</sup> species is involved in the dissociation of metastable [C<sub>6</sub>H<sub>5</sub>F·H<sup>+</sup>]. Ring-opening can indeed account for the medium component of the KER in that the internal energy of the system is reduced because of the increase of potential energy contained in the acyclic C<sub>6</sub>H<sub>5</sub><sup>+</sup> species. In addition, this isomerization path provides a rationalization for the ratios and the KIE between the medium and the broad components as well as the competing H<sub>2</sub> and HF losses for the metastable ions.

## Conclusions

Unimolecular dissociation of protonated fluorobenzene reveals quite complex behavior. In addition to the fragmentations of fluorine- and ring-protonated species reported earlier by Mason and co-workers,<sup>5,7</sup> the previous ab initio studies<sup>11</sup> as well as the RRKM theory treatment presented here suggest that there exist two different routes for elimination of HF from the ring-protonated forms. Moreover, fluorine insertion into the carbon skeleton is energetically conceivable for the metastable ions, thereby extending the range of possible isomers, e.g., fluorepinium. The present results also suggest the possibility of ring-opened C<sub>6</sub>H<sub>5</sub><sup>+</sup> species as one of the origins of the composite KER. Detailed consideration of C<sub>6</sub>H<sub>5</sub><sup>+</sup> species other than phenylium is rather difficult, however, because of the large number of isomers and the scarcity of experimental and theoretical data.

These limitations notwithstanding, the present study allows for an unambiguous assignment of the origin of the narrow and broad components of the KER associated with the unimolecular dehydrofluorination of fluorine- and ring-protonated fluorobenzene, respectively. Considering the limited knowledge on exit channel interactions of the diatomic HF with the remaining polyatomic phenyl cation, the agreement between the calculated and the measured KER is reasonably good. Moreover, the calculated rate coefficients and KERs can be used to discard the validity of the previously suggested<sup>11</sup> competition of 1,1- and 1,2-eliminations as a source of the different KERs. Circumstantial evidence in the interpretation of the KERs as well as the ion/molecule reactions suggest involvement of acyclic isomers. These species have higher potential energies (i.e., heat of formation), thereby reducing the amount of excess energy which is available for distribution in the rovibrational and translational modes of the ion. Thus, the previous statement that dehydrogenation of metastable [C<sub>6</sub>H<sub>5</sub>F·H<sup>+</sup>] involves three different routes must be modified. Three pathways give rise to phenylium ion and are associated with the broad and the narrow components of the KER. A fourth route leads to acyclic C<sub>6</sub>H<sub>5</sub><sup>+</sup> and gives rise to the medium component of the KER.

From a more general point of view, protonated fluorobenzenes provide valuable information on various aspects of the potential-energy surface of C<sub>6</sub>H<sub>5</sub><sup>+</sup> which displays considerable complexity and calls for further experimental and theoretical studies of this

fundamental species.<sup>12,34,44,45</sup> In fact, we believe that it is precisely the simplicity of the  $[\text{C}_6\text{H}_5\text{F}\cdot\text{H}^+]$  system which causes the complex fragmentation pattern due to the efficient competition of different pathways. More complex substrates, e.g., other halobenzenes or alkylated fluorobenzenes, would instead enhance the propensity for collapsing into a single, lowest-energy seam of the potential-energy surface which is then represented by a single isomer.

**Acknowledgment.** Financial support by the Deutsche Forschungsgemeinschaft, the Fonds der Chemischen Industrie, the Volkswagen-Stiftung, the Gesellschaft von Freunden der Technischen Universität Berlin, and the Funds for the Promotion of Research at the Technion is gratefully acknowledged. D.S. and H.S. also appreciate the hospitality of the Technion. In particular, we thank Professor Y. Apeloig, Technion, for helpful discussions and initiating the contact between the authors of this paper. Generous allocation of computing time by the Konrad Zuse Zentrum is gratefully acknowledged.

## Appendix I

The tenets of the statistical model are (i) the internal energy is statistically distributed among all the internal modes of the molecule. (ii) The source of the kinetic energy release, KER, comes only from the four transition modes and the reaction coordinate associated with the fragmentation. Energy from other modes does not contribute to the KER. The relevant modes associated with the reaction coordinate must be identified and their energy content is calculated. (iii) The KER is calculated by subtracting the rotational energy of the fragments from the available energy calculated in (ii).

The first assumption is that the molecular ion behaves ergodically and that it is large enough such that there is a microcanonical distribution of the internal energy with a characteristic vibrational–rotational temperature,  $T_v$ , obtained from the canonical expression

$$E = RT_v^2 \delta \ln Q / \delta T_v \quad (\text{A1})$$

where  $Q$  is the vibrational–rotational partition function and  $E$  is the total internal energy.

The second assumption is that as the ion dissociates only the energy in the modes directly associated with the fragmentation contribute to the KER. In the present case of the dissociation of the protonated fluorobenzene into a phenyl ion and an HF molecule, only four vibrations and the reaction coordinate are converted into translations, vibrations, and rotations of the products. The total available energy ( $E_{\text{avl}}$ ) for distribution is

$$E_{\text{avl}} = E_v + \Delta E_{\text{zp}} + E_b + E_{\text{rc}} \quad (\text{A2})$$

where  $E_v$  is the vibrational energy in the modes which contribute to the KER.  $\Delta E_{\text{zp}}$  is the difference between the zero point energy of the TS and the products.  $E_b$  is the energy of the barrier between the TS and the products.  $E_{\text{rc}}$  is the contribution of the energy in the reaction coordinate to the KER. The internal energy of each mode is given by

$$E_{v_i} = hv_i / (\exp(hv_i/kT_v) - 1) \quad (\text{A3})$$

where  $i$  indicates the  $i$ th mode. The value of  $E_v$  is then obtained by summing over all contributing modes

$$E_v = \sum_{i=1}^4 E_{v_i} \quad (\text{A4})$$

The value of  $E_{\text{rc}}$  is obtained by evaluating the average translational energy in the reaction coordinate

$$E_{\text{rc}} = \int_0^E \epsilon k(E, \epsilon) d\epsilon / \int_0^E k(E, \epsilon) d\epsilon \quad (\text{A5})$$

Here,  $k(E, \epsilon)$ , which is the energy dependent unimolecular rate coefficient per unit translational energy, is given by the RRKM theory expression

$$k(E, \epsilon) = \rho(E - \epsilon) / \rho(E') / h \quad (\text{A6})$$

where  $\rho(E - \epsilon)$  is the number of states with total energy  $E$  in the TS and translational energy  $\epsilon$  in the reaction coordinate and  $\rho(E')$  is the density of states at energy  $E'$ .

Integration of eq A6 over all values of the translational energy from 0 to  $E$  gives the well-known RRKM theory rate coefficient  $k(E) = \omega(E) / \rho(E') / h$ . Here,  $\omega(E)$  is the total number of states in the TS,  $\rho(E')$  is the density of states in the excited ion,  $h$  is Planck's constant, and  $E'$  is the internal energy.

The quantity  $\Delta E_{\text{zp}}$  is an important contribution and an integral part of the calculations of the KER since it takes care of the fact that all of the internal modes which convert into translations and rotations lose their zero-point energy that appears as rotation and translation.

The third tenet of the model requires the evaluation of the average rotational energy,  $\langle E_r \rangle$ . This energy is not available as translational energy and therefore the KER is given by the expression

$$\text{KER} = E_{\text{avl}} - \langle E_r \rangle \quad (\text{A7})$$

$\langle E_r \rangle$  was calculated by the expression

$$\langle E_r \rangle = \sum_{j=0}^{\infty} B j(j+1) F_r(j) \quad (\text{A8})$$

where  $B$  is the rotational constant.  $F_r(j)$ , the rotational distribution function, was calculated by two methods. One is a correlation of states for a two-dimensional harmonic oscillator-free rotor system and the other is a correlation of states for one-dimensional harmonic oscillator + one free rotor with states of a two-dimensional rotor. In the two-dimensional harmonic oscillator,  $F_r(j)$  is given by

$$F_r(j) = (1 - \lambda)[2\lambda^j - (1 + \lambda)\lambda^{2j}] \quad (\text{A9})$$

where  $\lambda = \exp(-h\omega_b/kT_v)$ . When equations (A8) and (A9) are combined, the final expression (A10) for the average rotational energy is obtained

$$\langle E_r \rangle = 2\lambda B [2 - \lambda / (1 + \lambda)^2] / (1 - \lambda)^2 \quad (\text{A10})$$

For the case of one harmonic oscillator and one free rotor, the distribution function is given by

$$F_r(j) = \sum_m F_r(j, m) \quad (\text{A11})$$

## Appendix II

Relative energies (at 0 K), moments of inertia, and harmonic molecular frequencies ( $\text{cm}^{-1}$ ) of the various species calculated with MP2/6-31G\*, for computational details, see ref 11. The letter D stands for the corresponding fully deuterated species  $\text{C}_6\text{D}_6\text{F}^+$ .

<b>1</b>	0.0 kcal/mol		339.5 GHz	720.3 GHz	1049.1 GHz								
	146	238	366	390	423	445	531	655	718	750	832	843	
	876	911	921	947	1024	1045	1061	1135	1145	1188	1284	1295	
	1349	1402	1485	2661	2672	2853	2861	2879	2881	cm <sup>-1</sup>			
<b>5</b>	57.4 kcal/mol		336.8 GHz	752.0 GHz	1081.0 GHz								
	187	284	341	381	419	505	526	574	620	687	724	856	
	882	898	912	930	936	973	1046	1059	1169	1238	1308	1322	
	1420	1445	1951	2862	2870	2873	2880	2882	cm <sup>-1</sup>				
<b>6</b>	59.2 kcal/mol		338.2 GHz	717.7 GHz	1043.7 GHz								
	205	270	370	413	428	513	538	602	669	708	761	806	
	886	898	911	927	956	991	1037	1059	1166	1229	1309	1323	
	1400	1461	1539	2778	2862	2871	2880	2884	cm <sup>-1</sup>				
<b>7</b>	20.7 kcal/mol		333.5 GHz	791.2 GHz	1119.4 GHz								
	165	169	247	284 <sup>a</sup>	376	383	505	549	567	647	655	714	
	807	818	875	906	914	944	950	1033	1049	1145	1189	1292	
	1330	1384	1525	2860	2865	2878	2892	2892	3301	cm <sup>-1</sup>			
<sup>a</sup> The mode at 284 cm <sup>-1</sup> was taken as the reaction coordinate for the dissociation of 7.													
<b>1-D</b>	0.0 kcal/mol		420.2 GHz	784.7 GHz	1183.4 GHz								
	123	205	332	348	359	433	506	509	592	654	677	680	
	733	758	764	782	798	805	809	847	926	1078	1145	1269	
	1329	1347	1454	1942	1969	2108	2114	2134	2138	cm <sup>-1</sup>			
<b>5-D</b>	58.5 kcal/mol		408.3 GHz	824.6 GHz	1218.0 GHz								
	175	260	296	342	378	404	477	504	545	568	594	689	
	713	721	736	766	767	777	843	882	917	1170	1211	1238	
	1372	1415	1453	2113	2120	2126	2137	2139	cm <sup>-1</sup>				
<b>6-D</b>	60.6 kcal/mol		410.6 GHz	787.5 GHz	1181.0 GHz								
	194	229	329	367	381	457	506	524	543	567	653	657	
	711	714	732	767	771	774	848	900	920	1104	1188	1202	
	1257	1366	1466	2052	2114	2123	2135	2140	cm <sup>-1</sup>				

## References and Notes

- (1) Kuck, D. *Mass Spectrom. Rev.* **1990**, *9*, 187 and 583.
- (2) Mason, R. S.; Williams, C. M.; Anderson, P. D. *J. Chem. Soc., Chem. Commun.* **1995**, 1027.
- (3) Glukhovtsev, M. N.; Pross, A.; Nicolaidis, A.; Radom, L. *J. Chem. Soc., Chem. Commun.* **1995**, 2347.
- (4) DePuy, C. H.; Gareyev, R.; Fornarini, S. *Int. J. Mass Spectrom. Ion Processes* **1997**, *161*, 41.
- (5) Mason, R. S.; Fernandez, M. T.; Jennings, K. R. *J. Chem. Soc., Faraday Trans.* **1987**, *83*, 89.
- (6) Tkaczyk, M.; Harrison, A. G. *Int. J. Mass Spectrom. Ion Processes* **1994**, *132*, 73.
- (7) Mason, R. S.; Parry, A. J.; Milton, D. M. P. *J. Chem. Soc., Faraday Trans.* **1994**, *90*, 1373.
- (8) Mason, R. S.; Milton, D. M. P.; Harris, F. *J. Chem. Soc., Chem. Commun.* **1987**, 1453.
- (9) Maksic, Z. B.; Eckert-Maksic, M.; Klessinger, M. *Chem. Phys. Lett.* **1996**, *260*, 572.
- (10) Szulejko, J. E.; Hrušák, J.; McMahon, T. B. *J. Mass Spectrom.* **1997**, *32*, 494.
- (11) Hrušák, J.; Schröder, D.; Weiske, T.; Schwarz, H. *J. Am. Chem. Soc.* **1993**, *115*, 2015.
- (12) Eyler, J. R.; Campana, J. E. *Int. J. Mass Spectrom. Ion Processes* **1983/1984**, *55*, 171.
- (13) Cooks, R. G.; Beynon, J. H.; Caprioli, R. M.; Lester, G. R. *Metastable Ions*; Elsevier: Amsterdam, 1973.
- (14) Derrick, P. J.; Donchi, K. F. In *Comprehensive Chemical Kinetics*; Bamford, C. H., Tipper, C. F. H., Eds.; Elsevier: Amsterdam, 1983; Vol. 24, p 53.
- (15) Holmes, J. L.; Osborne, A. D. *Int. J. Mass Spectrom. Ion Phys.* **1977**, *23*, 189.
- (16) Nikitin, E. E. *Theory of Elementary Atomic and Molecular Processes in Gases*; Clarendon: Oxford, 1974.
- (17) Quack, M.; Troe, J. In *Statistical Methods in Scattering in Theoretical Chemistry: Theory of Scattering*; Henderson, D., Ed.; Academic Press: New York, 1981.
- (18) Nikitin, E. E.; Troe, J. *J. Chem. Phys.* **1990**, *92*, 6594.
- (19) Callear, A. B. In *Comprehensive Chemical Kinetics*; Bamford, C. H., Tipper, C. F. H., Eds.; Elsevier: Amsterdam, 1983; Vol. 24, p 333.
- (20) Srinivas, R.; Sülzle, D.; Weiske, T.; Schwarz, H. *Int. J. Mass Spectrom. Ion Processes* **1991**, *107*, 368.
- (21) Srinivas, R.; Sülzle, D.; Koch, W.; DePuy, C. H.; Schwarz, H. *J. Am. Chem. Soc.* **1991**, *113*, 5970.
- (22) Schalley, C. A.; Schröder, D.; Schwarz, H. *Int. J. Mass Spectrom. Ion Processes* **1996**, *153*, 173.
- (23) Busch, K. L.; Glish, G. L.; McLuckey, S. A. *Mass Spectrometry/ Mass Spectrometry: Techniques and Applications of Tandem Mass Spectrometry*; VCH: Weinheim, 1988.
- (24) Schröder, D.; Schwarz, H. *Int. J. Mass Spectrom. Ion Processes* **1995**, *146/147*, 183.

- (25) Eller, K.; Schwarz, H. *Int. J. Mass Spectrom. Ion Processes* **1989**, *93*, 243.
- (26) Eller, K.; Zummack, W.; Schwarz, H. *J. Am. Chem. Soc.* **1990**, *112*, 621.
- (27) Freiser, B. S. *Chemtracts: Anal. Phys. Chem.* **1989**, *1*, 65.
- (28) Fiedler, A.; Kretzschmar, I.; Schröder, D.; Schwarz, H. *J. Am. Chem. Soc.* **1996**, *118*, 9941.
- (29) Schröder, D.; Schwarz, H.; Clemmer, D. E.; Chen, Y.-M.; Armentrout, P. B.; Baranov, V. I.; Böhme, D. K. *Int. J. Mass Spectrom. Ion Processes* **1997**, *161*, 177.
- (30) Proton affinities were taken from: Hunter, E. P. L.; Lias, S. G. *J. Phys. Chem. Ref. Data* **1998**, *27*, 413.
- (31) Heinemann, C.; Schröder, D.; Schwarz, H. *J. Phys. Chem.* **1995**, *99*, 16195.
- (32) Schröder, D.; Schalley, C. A.; Harvey, J. N.; Schwarz, H. *Int. J. Mass Spectrom.* **1999**, *185–187*, 25.
- (33) Bohme, D. K.; Stone, J. A.; Mason, R. S.; Stradling, R. S.; Jennings, K. R. *Int. J. Mass Spectrom. Ion Phys.* **1981**, *37*, 283.
- (34) Speranza, M.; Sefcik, M. D.; Henis, J. M. S.; Gaspar, P. P. *J. Am. Chem. Soc.* **1977**, *99*, 5583.
- (35) Burgers, P. C.; Holmes, J. L. *Int. J. Mass Spectrom. Ion Processes* **1984**, *58*, 15.
- (36) Rumpf, B. A.; Allison, C. E.; Derrick, P. J. *Org. Mass. Spectrom.* **1986**, *21*, 295.
- (37) More precisely, for  $k = 10^5 \text{ s}^{-1}$  an internal energy of 86.0 kcal/mol is required for dissociation via **5** and 90.5 kcal/mol for dissociation via **6**. Likewise,  $k = 3 \times 10^5 \text{ s}^{-1}$  corresponds to internal energies of 91.0 and 95.5 kcal/mol, respectively. For  $[\text{C}_6\text{D}_5\text{F}\cdot\text{D}^+]$ , the corresponding energies are 93.5 and 99.0 kcal/mol for  $k = 10^5 \text{ s}^{-1}$  and 98.5 and 104.0 kcal/mol for  $k = 3 \times 10^5 \text{ s}^{-1}$ , respectively.
- (38) Thibblin, A.; Ahlberg, P. *Chem. Soc. Rev.* **1989**, *18*, 209.
- (39) See p 84–87 in ref 14.
- (40) Holmes, J. L.; Terlouw, J. K. *Org. Mass Spectrom.* **1980**, *15*, 383.
- (41) Bernardi, F.; Grandinetti, F.; Guarino, A.; Robb, M. A. *Chem. Phys. Lett.* **1988**, *153*, 309.
- (42) Gasper, S. M.; Devadoss, C.; Schuster, G. B. *J. Am. Chem. Soc.* **1995**, *117*, 5206.
- (43) See also: Logan, C. F.; Chen, P. *J. Am. Chem. Soc.* **1996**, *118*, 2113.
- (44) Hrušák, J.; Schröder, D.; Iwata, S. *J. Chem. Phys.* **1997**, *106*, 7541.
- (45) Nicolaides, A.; Smith, D. M.; Jensen, F.; Radom, L. *J. Am. Chem. Soc.* **1997**, *119*, 8083.
- (46) Aschi, M.; Harvey, J. N.; Schalley, C. A.; Schröder, D.; Schwarz, H. *J. Chem. Soc., Chem. Commun.* **1998**, 531.
- (47) Hrušák, J. *Theor. Chim. Acta* **1990**, *78*, 209.
- (48) Tajima, S.; Ueki, M.; Tajima, S.; Sekiguchi, O.; Shigihara, A. *Rapid Commun. Mass Spectrom.* **1996**, *10*, 1076.
- (49) Dewar, M. J. S.; Gardiner, W. C., Jr.; Frenlach, M.; Oref, I. *J. Am. Chem. Soc.* **1987**, *109*, 4456.
- (50) Huang, J. H.; Han, K.-L.; Deng, W.-Q.; He, G.-Z. *Chem. Phys. Lett.* **1997**, *273*, 205.
- (51) According to a recent theoretical treatment, triplet phenylium  $\text{C}_6\text{H}_5^+$  ( $^3\text{B}_2$ ) cannot be monitored in these experiments because its unimolecular lifetime is predicted to be short ( $\mu\text{s}$ ) due to rapid intersystem crossing to the singlet surface, see ref 52.
- (52) Harvey, J. N.; Aschi, M.; Schwarz, H.; Koch, W. *Theor. Chem. Acc.* **1998**, *99*, 95.
- (53) Also, charge reversal of  $\text{C}_6\text{H}_5^+$  cations can be used to probe the presence of acyclic isomers, see: Schröder, D.; Schroeter, K.; Zummack, W.; Schwarz, H. *J. Am. Soc. Mass Spectrom.*, in press.
- (54) Lias, S. G.; Bartmess, J. E.; Liebman, J. F.; Holmes, J. L.; Levin, R. D.; Mallard, W. G. *Gas-Phase Ion and Neutral Thermochemistry*, *J. Phys. Chem. Ref. Data, Suppl. 1* **1988**, *17*.
- (55) Butcher, V.; Costa, M. L.; Dyke, J. M.; Ellis, A. R.; Morris, A. *Chem. Phys.* **1987**, *115*, 261.
- (56) For example, the PAs of the 2-halotoluenes are 185 (X = F), 189 (X = Cl), 185 (X = Br), and 187 (X = I) kcal/mol; see ref 30.
- (57) Hertwig, R. H.; Koch, W.; Schröder, D.; Schwarz, H.; Hrušák, J.; Schwerdtfeger, P. *J. Phys. Chem.* **1996**, *100*, 12253.
- (58) Schröder, D.; Schwarz, H.; Hrušák, J.; Pyykkö, P. *Inorg. Chem.* **1998**, *37*, 624.